UDC 621.7 **doi: 10.20998/2078-7405.2025.103.04**

# INFLUENCE OF MACHINING-BASED POST-PROCESSING ON THE SURFACE TOPOGRAPHY OF DMLS 316L STAINLESS STEEL FOR FUSION-RELEVANT APPLICATIONS

István **Sztankovics**[1*] [0000-0002-1147-7475], Gábor **Veres**[2,3] [0009-0000-0708-9405], Csaba **Felhő**[1] [0000-0003-0997-666X], Antal **Nagy**[1] [0000-0001-6160-4973], Péter **Figeczki-Mélykuti**[2] [0009-0001-5454-0913]

[1]Institute of Manufacturing Science, University of Miskolc, H-3515, Miskolc – Egyetemváros, Hungary
[2] HUN-REN Centre for Energy Research, H-1121 Budapest, Konkoly-Thege Miklós út 29-33., Hungary
[3] Institute of Nuclear Technics, Budapest University of Technology and Economics, H-1111 Budapest, Műegyetem rkp. 3., Hungary
[*] istvan.sztankovics@uni-miskolc.hu

**Received: 10 November 2025/ Revised: 19 November 2025/ Accepted: 29 November 2025 / Published: 15 December 2025**

**Abstract.** *This study investigates the effect of machining-based post-processing on the surface topography of Direct Metal Laser Sintered (DMLS) 316L stainless steel intended for fusion-relevant applications. Cubic samples (30 × 30 × 30 mm) were produced by additive manufacturing and subsequently finished by face milling and surface grinding under two parameter settings each. The surface topography was characterized using an AltiSurf 520 optical system in accordance with ISO 25178. The as-printed surface exhibited high roughness ($S_a$ = 8.899 µm, $S_z$ = 79.427 µm), while all post-processed surfaces showed significant improvements. The lowest roughness ($S_a$ = 1.346 µm) was obtained after grinding at 7 m/min feed rate. Skewness and kurtosis analysis indicated that machining transformed the peak-dominated surface into a more uniform, near-Gaussian texture. The results confirm that controlled milling and grinding operations can effectively enhance the surface integrity of DMLS 316L components. These findings demonstrate the potential of hybrid additive–subtractive manufacturing to produce surfaces suitable for the vacuum and functional requirements of fusion technology applications.*
**Keywords:** *additive manufacturing; DMLS 316L stainless steel; surface topography; post-processing; fusion technology applications.*

## 1. Introduction

Additive manufacturing (AM) has emerged as one of the most transformative technologies in modern engineering, enabling the production of complex components with high design freedom and material efficiency [1,2]. Among the various AM techniques, Direct Metal Laser Sintering (DMLS) has gained particular importance for producing metallic components with intricate geometries that are

difficult or impossible to fabricate using traditional subtractive manufacturing methods [3,4]. In DMLS, a high-energy laser beam selectively melts fine layers of metallic powder, such as stainless steel, titanium, or nickel-based alloys, to build a part layer by layer directly from a digital model. This layer-wise approach allows for the realization of lightweight structures, internal channels, and functional gradients that are highly advantageous for advanced engineering applications [5-8]. However, despite these benefits, DMLS parts often exhibit intrinsic challenges, such as high surface roughness, porosity, and residual stresses, which can limit their use in critical technological environments [9,10].

One of the most promising areas for applying additive manufacturing is the field of fusion technology [11]. In experimental fusion devices and future reactors, such as ITER and DEMO, component design must meet demanding mechanical, thermal, and vacuum performance criteria [12,13]. The extreme conditions inside the fusion environment – characterized by high temperatures, cyclic thermal loads, radiation exposure, and ultra-high vacuum – place strict constraints on material selection and manufacturing quality. Structural and functional components within the vacuum chamber must not only maintain mechanical integrity but also exhibit low outgassing rates and high surface density to ensure vacuum compatibility [14,15]. Any surface irregularities, porosity, or contamination can significantly impair vacuum tightness and introduce sources of gas emission, thereby compromising operational stability. Therefore, before AM parts can be reliably implemented in fusion systems, their surface and subsurface characteristics must be optimized to meet these stringent requirements.

316L stainless steel is among the most widely used materials for both additive and conventional fabrication of components in vacuum and fusion environments [16,17]. It combines good mechanical strength, corrosion resistance, and non-magnetic properties with excellent weldability. When processed through DMLS, 316L retains these beneficial features but often exhibits a characteristic rough, layered surface and microstructural inhomogeneity [18,19]. These as-built surface conditions are typically unsuitable for vacuum applications, where smoothness and compactness are crucial for ensuring adequate sealing and minimizing gas entrapment. Therefore, appropriate post-processing methods must be employed to refine the surface topography, eliminate near-surface defects, and improve functional performance.

Machining-based post-processing methods, such as face milling and face grinding, represent practical and effective approaches for improving the surface quality of additively manufactured metal components [8,20]. These techniques enable the controlled removal of the rough outer layers, reducing waviness, asperity peaks, and partially melted particles originating from the DMLS process. The resulting modifications in surface topography can significantly influence the mechanical behaviour, wear resistance, and vacuum performance of the components.

However, the interaction between the machined surface and the underlying additively manufactured microstructure remains complex, as the anisotropy, porosity, and hardness variations within DMLS parts may affect machining efficiency and surface finish outcomes [21,22]. Consequently, systematic evaluation of machining-based post-processing is necessary to identify optimal processing parameters that produce surfaces suitable for fusion-related applications.

Recent literature demonstrates that post-processing is essential to render DMLS 316L surfaces suitable for demanding applications. Powder-bed fusion parts typically show high as-built roughness, partially fused particles and near-surface porosity, which can degrade fatigue performance and surface-dependent functional properties; several studies quantify these effects and show that controlled machining or polishing substantially reduces roughness and improves fatigue and breakdown behaviour [16,23]. Experimental and review papers indicate machining and other mechanical finishing methods are effective at removing the superficial, layer-induced defects, while thermal or HIP treatments can additionally close internal porosity and homogenize microstructure when required [9,24]. Importantly for fusion or accelerator vacuum applications, recent targeted evaluations found that DMLS 316L can achieve ultra-high vacuum suitability after appropriate post-processing and baking steps, with some machined samples reaching leak rates near instrument detection limits and showing pump-down behaviour comparable to wrought material [25]. Taken together, these studies motivate systematic comparisons of machining routes such as face milling and face grinding on DMLS 316L to identify parameter sets that reliably produce surface topographies compatible with fusion-relevant requirements.

The present study addresses this challenge by investigating the influence of face milling and face grinding on the surface topography of DMLS 316L stainless steel specimens. By analysing different machining parameters and quantifying their effects on areal roughness characteristics, the study aims to assess the suitability of post-processed DMLS parts for use in fusion environments. The findings contribute to defining process–structure–surface relationships that can guide the future qualification of additively manufactured metallic components in fusion technology.

## 2. Experimental conditions and methods

Additive manufacturing experiments were carried out using 316L stainless steel specimens produced by Direct Metal Laser Sintering (DMLS). The printing process was performed at VARINEX Zrt. using 316L stainless steel powder. The parts were manufactured in the form of small cubic samples with nominal dimensions of 30 × 30 × 30 mm. A total of five samples were produced to allow systematic comparison of different machining-based post-processing conditions. The DMLS-made parts were divided into five groups: one as-printed reference and

four samples subjected to different post-processing combinations of milling and grinding parameters. The aim of this setup was to characterize the influence of machining conditions on the resulting surface topography and to identify trends in surface modification achievable through mechanical finishing. The samples were subjected to two distinct machining methods: face milling and longitudinal peripheral plane grinding. Both techniques were selected because of their industrial relevance and their different material removal mechanisms, which allow a comparative understanding of surface formation in additively manufactured metallic materials.

The face milling operations were performed on a Perfect Jet MCV-M8 vertical machining centre. The tool assembly consisted of a Tungaloy T2845 PM 063.05Z5W tool holder equipped with a BFT Burzoni OFEX 05T3AE cutting insert. The insert was manufactured from KH100-grade carbide, providing sufficient wear resistance and edge stability when cutting stainless steel. During the experiments, one insert was clamped into the toolholder. Milling was carried out under flooded lubrication using CIKS HKF 420 coolant to minimize temperature rise and to assist chip evacuation. Two parameter combinations were investigated for the milling process: both employed a cutting speed of 200 m/min and a constant depth of cut of 0.5 mm, while the feed per tooth ($f_z$) was varied between 0.5 mm/rev and 0.8 mm/rev. This variation allowed the assessment of feed influence on the surface texture and material removal characteristics.

The grinding operations were conducted on a Metallkraft FSM 4080 precision surface grinding machine, which ensured high rigidity and fine controllability of process parameters. A grinding wheel with an outer diameter of 343.4 mm was used. The process was performed under flooded cooling with the same CIKS HKF 420 coolant to maintain consistent lubrication and thermal conditions across both machining technologies. For grinding, the main process parameters included a rotational speed of 1450 RPM, a depth of cut of 0.05 mm, and a stroke width of 1.5 mm per pass. The feed rate ($v_f$) was varied at two levels, 7 m/min and 9 m/min, to evaluate its effect on the achieved surface topography. These conditions were chosen to represent typical fine-finishing operations applicable to stainless steel components.

As a result, the complete set of experiments included five surface conditions: one as-printed, two milled, and two ground surfaces. After machining, all samples underwent careful cleaning to remove coolant residues and any loosely adhered particles. No heat treatment, density testing, or vacuum qualification procedures were carried out in the present phase of the study, but these investigations are planned as part of future work to establish correlations between surface finish and vacuum compatibility. Similarly, detailed microscopic analyses, including optical or scanning electron microscopy, are also intended for the next research stage to complement the quantitative topography measurements.

Surface characterization was performed using an AltiSurf 520 three-dimensional topography measurement system. This instrument enables non-contact areal surface measurement based on optical scanning principles, providing high-resolution topographic data suitable for areal roughness parameter evaluation. The surface measurements were analysed using the AltiMap Premium v6.2.7487 software package. Each sample was measured once over an area of 4 × 4 mm, with a resolution of 1 μm times 10 μm. The evaluation of the acquired surface data followed the ISO 25178 standard for areal surface texture analysis, which allows the quantification of both amplitude and functional characteristics of surface morphology. The parameters investigated in this study included the arithmetic mean height ($S_a$), maximum height ($S_z$), skewness ($S_{sk}$), and kurtosis ($S_{ku}$). These parameters collectively describe the average roughness, the extreme height difference, and the statistical distribution of surface peaks and valleys, offering comprehensive insight into the effectiveness of post-processing operations. No averaging or statistical repetition was applied at this stage, as the study aimed primarily to identify qualitative trends and establish methodological feasibility for subsequent, more extensive experiments.

The selected methodology ensures that the observed differences in surface topography can be directly attributed to the applied machining conditions. By maintaining consistent coolant, tool, and machine configurations, while varying only the feed per tooth or feed rate, the influence of process dynamics on the surface structure of DMLS 316L stainless steel can be systematically assessed. The combination of high-precision surface measurement and controlled machining conditions provides a robust basis for understanding how additive manufactured surfaces respond to traditional subtractive finishing. The obtained data serve as the foundation for developing optimized post-processing protocols that could make additively manufactured stainless steel components suitable for integration into fusion-relevant environments, where both surface quality and structural integrity are of critical importance.

## 3. Results and Discussion

The corresponding quantitative roughness parameters extracted from the areal measurements are summarized in Table 1: the arithmetical mean height ($S_a$), the maximum height ($S_z$), the skewness ($S_{sk}$), and the kurtosis ($S_{ku}$).

Table 1 – Summary of the surface roughness measurement results

| Process | 3D printed | Milling 0.5 mm/rev. | Milling 0.8 mm/rev. | Grinding 7m/min | Grinding 9 m/min |
|---|---|---|---|---|---|
| $S_a$ [μm] | 8.899 | 1.726 | 2.244 | 1.346 | 1.666 |
| $S_z$ [μm] | 79.427 | 10.246 | 13.936 | 12.045 | 19.023 |

| | | | | | |
|---|---|---|---|---|---|
| $S_{sk}$ [-] | 0.147 | -0.168 | 0.308 | -0.261 | -0.487 |
| $S_{ku}$ [-] | 3.090 | 1.925 | 1.922 | 2.927 | 3.305 |

Figure 1 presents the representative 3D surface topography maps obtained from each surface preparation method: (a) as-printed, (b) milling with 0.5 mm/rev feed, (c) milling with 0.8 mm/rev feed, (d) grinding at 7 m/min, and (e) grinding at 9 m/min.

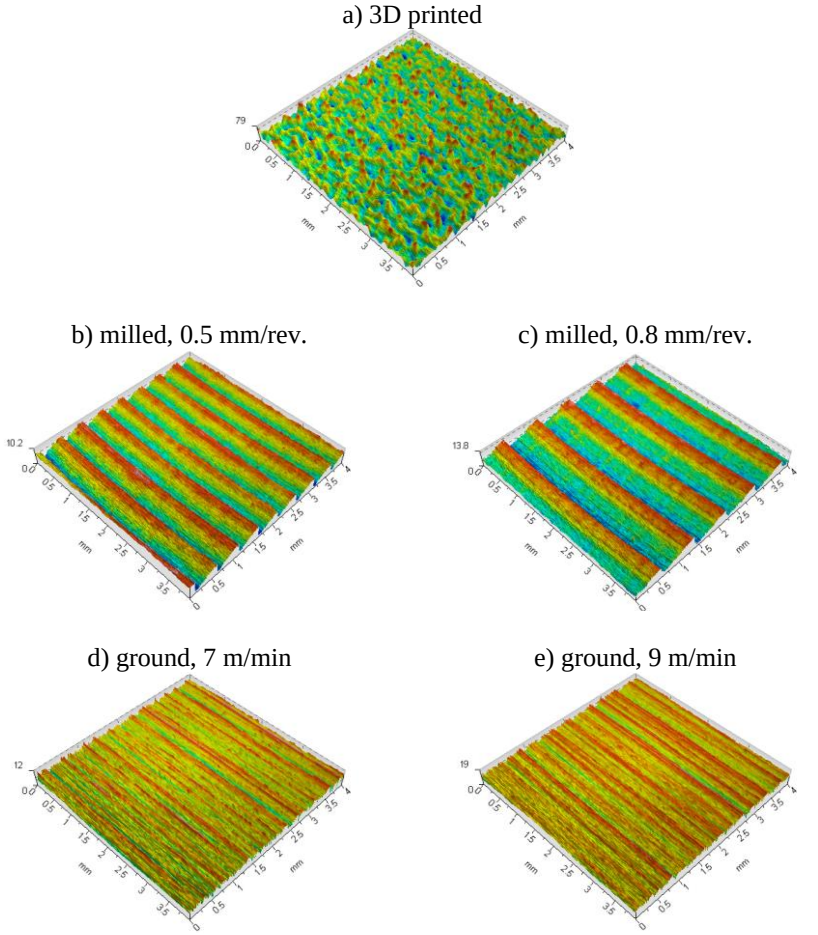


Figure 1 – Variation of the Average Height of the Waviness profile in the studied range

### 3.1 General trends and surface morphology

The surface topographies reveal a clear transition from the highly irregular and layered morphology of the 3D printed surface to smoother and more uniform textures obtained after milling and grinding. The as-printed surface exhibits pronounced waviness and asperities, resulting from the layer-by-layer deposition inherent in the additive manufacturing process. These height variations are quantitatively reflected in its $S_a$ value of 8.899 μm and $S_z$ value of 79.427 μm, both significantly higher than those of any of the subsequent subtractive processes. Such values are characteristic of typical fused deposition or powder-bed printed metallic or polymeric surfaces, where partially melted particles, stair-step effects, and inter-layer ridges dominate the microgeometry.

When the printed surfaces were subjected to milling and grinding, substantial reductions in both $S_a$ and $S_z$ were observed, confirming the strong smoothing effect of material removal. Among the milled samples, the surface milled at a lower feed of 0.5 mm/rev achieved the smallest $S_a$ value (1.726 μm), while the higher feed of 0.8 mm/rev resulted in a slightly rougher texture ($S_a$ = 2.244 μm). This trend is consistent with general machining theory, as higher feed per revolution increases the uncut chip thickness and the feed marks left by the cutting tool, thereby amplifying the surface roughness amplitude. Nevertheless, both milled surfaces exhibit an order-of-magnitude reduction in $S_a$ compared to the as-printed sample, demonstrating the capability of milling to significantly improve surface quality in post-processing of additively manufactured parts.

The ground surfaces further improved smoothness, reaching $S_a$ values of 1.346 μm and 1.666 μm for the 7 m/min and 9 m/min cutting speeds, respectively. The lower feed rate thus provided the finest finish, consistent with the notion that slower feed rates in abrasive processes generally allow for more controlled material removal and reduced thermal damage. The slightly higher roughness at 9 m/min may be attributed to increased thermal softening or local wheel loading, which can alter the effective cutting edges and cause ploughing rather than pure abrasion. Despite these differences, both grinding conditions resulted surfaces with $S_a$ below 2 μm, marking a substantial refinement compared with the printed and milled conditions.

### 3.2 Amplitude parameters

The evolution of $S_a$ and $S_z$ values across the five setups reveals the dominant role of surface generation mechanisms in determining the overall amplitude characteristics. The highest values observed in the printed sample ($S_a$ = 8.899 μm, $S_z$ = 79.427 μm) confirm the presence of tall peaks and deep valleys. The ratio between $S_z$ and $S_a$ is approximately 8.9, suggesting that extreme height features significantly contribute to the overall texture, a common feature of layer-based manufacturing. The subsequent milling and grinding processes not only reduced the average height deviations but also compressed the peak-to-valley range, leading to $S_z$ values between 10.246 and 19.023 μm.

A closer comparison of the milling results indicates that increasing feed from 0.5 to 0.8 mm/rev raised $S_z$ from 10.246 to 13.936 μm, a roughly 36% increase, which aligns with the increased feed mark depth and the larger cusp height expected from a coarser toolpath spacing. However, even the rougher milled surface exhibits an $S_z$ value that is only about one-sixth of that of the printed surface, highlighting the remarkable flattening effect of milling.

Grinding introduced another level of surface refinement. The lowest $S_z$ value (12.045 μm) was achieved at 7 m/min, while the higher feed rate (9 m/min) produced a noticeably higher $S_z$ of 19.023 μm. This indicates that increasing the wheel speed may promote instability in the contact zone, potentially due to thermal effects or insufficient coolant efficiency. Such sensitivity of $S_z$ to process parameters emphasizes the need for optimized grinding conditions when targeting ultra-smooth functional surfaces.

Overall, both $S_a$ and $S_z$ parameters follow the expected trend: 3D printing > milling (0.8 mm/rev) > milling (0.5 mm/rev) > grinding (9 m/min) > grinding (7 m/min), demonstrating the progressive improvement of surface finish through successive mechanical removal steps.

### 3.3 Material distribution parameters

While $S_a$ and $S_z$ describe the amplitude of surface deviations, the skewness and kurtosis provide insight into the shape of the height distribution, revealing whether the surface is dominated by peaks or valleys, and whether it has sharp or flat features. These parameters are crucial for predicting the tribological and functional performance of surfaces, such as bearing capacity, lubrication retention, and contact behaviour.

The as-printed surface shows a slightly positive skewness ($S_{sk}$ = 0.147), suggesting a peak-dominated structure where asperities project above the mean plane. This morphology is typical for additively manufactured parts, in which partially fused particles and ridges create a surface rich in isolated high spots. Such peak-dominated textures can lead to poor contact conformity and rapid wear if used in sliding applications without post-processing.

After milling, the $S_{sk}$ values changed notably. At 0.5 mm/rev, $S_{sk}$ became slightly negative (-0.168), while at 0.8 mm/rev it turned positive again (0.308). This alternating behaviour indicates that feed rate significantly affects the distribution of peaks and valleys. The lower feed produced a surface with shallow valleys and flattened peaks, as cutting marks overlap and the tool removes more irregularities per revolution. In contrast, the higher feed increased the tendency toward periodic ridges, reintroducing a peak-dominated profile. These results underline the strong geometric influence of feed per revolution on the material distribution and texture symmetry in milled surfaces.

Grinding further shifted the skewness toward negative values, with $S_{sk}$ equal to -0.261 at 7 m/min and -0.487 at 9 m/min. This indicates valley-dominated surfaces, where the material removal preferentially smooths the high peaks and leaves a plateau structure with residual micro-depressions. Such surfaces are advantageous for functional applications requiring lubricant retention or improved load distribution, as the valleys can serve as micro-reservoirs. The increasingly negative $S_{sk}$ at higher feed rate suggests more pronounced valley features, which might be associated with localized material pull-out or micro-grooving caused by abrasive interactions.

The kurtosis values ($S_{ku}$) complement this analysis by indicating the sharpness or flatness of the height distribution. An ideal Gaussian surface has $S_{ku}$ = 3, while values below 3 imply a broader, flatter distribution and values above 3 correspond to sharp, spiky textures. The printed surface shows $S_{ku}$ = 3.090, nearly Gaussian but slightly peaked, consistent with its heterogeneous and irregular asperity structure. The milled surfaces, however, display markedly lower $S_{ku}$ values (1.925 and 1.922), indicating flatter, more uniform height distributions. This suggests that milling effectively homogenized the surface texture, reducing the occurrence of extreme peaks or valleys.

In contrast, grinding at both speeds increased $S_{ku}$ to 2.927 and 3.305, respectively. The first case (7 m/min) is still near-Gaussian, implying a balanced texture with moderate peaks and valleys, while the second (9 m/min) clearly shows a more peaked distribution, possibly due to fine grooves or abrasive scratches that introduce localized height variations. The combined $S_{sk}$ and $S_{ku}$ trends indicate that grinding tends to produce negatively skewed, moderately peaked surfaces, favourable for tribological applications where controlled valleys improve lubricant flow, but sharp asperities are undesirable.

### 3.4 Comparative evaluation and functional implications

The combined analysis of amplitude and distribution parameters reveals that each surface preparation method produces a distinct topographical signature, directly influencing the potential functional performance. The 3D printed surface, while structurally sound, exhibits the roughest and most irregular morphology, making it unsuitable for precision mechanical contact or sealing applications without post-processing. Its high $S_a$ and $S_z$ values, together with a slightly positive skewness, imply limited bearing area and increased risk of high local contact stresses.

Milling effectively removes these irregularities, producing surfaces with $S_a$ below 2.5 μm and balanced $S_{sk}$ and $S_{ku}$ values, particularly at the lower feed rate. The smoother, more isotropic character achieved at 0.5 mm/rev indicates that controlled feed selection can yield near-Gaussian surfaces with improved uniformity. Such textures are well suited for applications requiring moderate friction and wear resistance, as the absence of pronounced peaks minimizes abrasive interactions.

However, the milled surfaces remain slightly directional due to feed marks, as evident from the anisotropic features seen in Figure 1(b–c).

Grinding offers the finest finish and the most functionally advantageous surface structure. The lower-speed grinding condition (7 m/min) produced the best combination of parameters, with low $S_a$ and $S_z$, negative $S_{sk}$, and near-Gaussian $S_{ku}$. This indicates a plateau-like surface with shallow valleys, ideal for applications requiring both smoothness and lubricant retention. Increasing the feed rate to 9 m/min, although still resulting in a relatively fine surface, introduced slightly higher roughness and stronger negative skewness, possibly linked to thermal or wheel–workpiece interaction effects. The findings thus highlight the need to balance process speed and surface integrity in grinding operations, as excessive speed may compromise topographical uniformity.

### 3.5 Correlation between roughness parameters and process characteristics

The strong correlation between process kinematics and topographical outcomes can be further discussed in terms of material removal mechanisms. In additive manufacturing, surface roughness is primarily determined by melt pool dynamics and powder or filament deposition accuracy, resulting in large-scale irregularities. Milling, dominated by mechanical shearing and chip formation, produces periodic feed marks that depend on the tool geometry and feed per revolution. Grinding, on the other hand, involves micro-scale cutting by abrasive grains, which generates random, isotropic micro-features.

These mechanisms explain the observed progression of $S_a$ and $S_z$ reductions and the corresponding shifts in $S_{sk}$ and $S_{ku}$. The printed surface peak-dominated texture (positive $S_{sk}$) arises from deposited ridges, while the milled surfaces exhibit transitional behavior where tool–material interaction alternates between cutting and ploughing, depending on feed rate. Finally, the ground surfaces achieve valley-dominated distributions (negative $S_{sk}$) due to abrasive flattening of asperities. The variation in $S_{ku}$ values reinforces this interpretation, as flatter distributions occur when material removal is stable and uniform, while peaked distributions reflect localized irregularities.

### 3.6 Summary of findings

The comparative results demonstrate that both milling and grinding are effective for post-processing additively manufactured surfaces, yet they differ in their ability to modify surface characteristics. Milling significantly improves roughness by removing macro-scale irregularities, but its texture remains influenced by toolpath geometry and feed rate. Grinding achieves finer finishes and more favorable material distributions, producing plateau-like surfaces beneficial for tribological performance. Quantitatively, the total reduction in $S_a$ from 8.899 μm

(printed) to 1.346 μm (ground, 7 m/min) represents an 85% improvement in mean height, while $S_z$ decreased by approximately 85% as well, confirming a consistent leveling of the surface profile. The accompanying evolution of $S_{sk}$ from positive to negative values and $S_{ku}$ toward near-Gaussian levels indicates an overall transition from irregular, peak-rich to uniform, valley-balanced textures.

## 5. Conclusions

This preliminary investigation examined the surface topography of additively manufactured components and their post-processed counterparts produced by milling and grinding. Quantitative 3D surface measurements revealed substantial improvements in surface quality after subtractive finishing operations. The as-printed surfaces exhibited high roughness amplitudes ($S_a$ = 8.899 μm, $S_z$ = 79.427 μm) and a slightly positive skewness, indicating a peak-dominated morphology typical of layer-based fabrication. Subsequent machining operations significantly reduced surface irregularities, confirming their suitability for enhancing the functional properties of 3D printed parts. Among the post-processing methods, milling with a feed of 0.5 mm/rev and grinding at a feed rate of 7 m/min produced the smoothest and most uniform surfaces. These conditions resulted in the lowest $S_a$ values (1.726 μm and 1.346 μm, respectively) and near-Gaussian height distributions. Grinding generated negatively skewed textures characterized by shallow valleys and plateau structures, which are advantageous for applications involving friction, lubrication, or wear contact. The results demonstrated that controlled finishing parameters allow a transition from rough, peak-dominated printed textures to refined, valley-balanced surfaces suitable for functional testing and potential industrial application. The findings indicate that 3D printed parts, when properly finished, can meet the surface quality requirements necessary for the intended purpose of the ongoing research project. The printed base material provided a stable substrate, and the achieved surface characteristics after milling and grinding suggest that additive–subtractive hybrid manufacturing can effectively combine geometric flexibility with surface precision. In this context, the study confirms the viability of integrating 3D printing as a preparatory step in producing components that require specific surface functionality after finishing.

However, as this was a preliminary study, further investigations are needed to fully validate the process chain and to explore the influence of additional variables such as tool geometry, cutting speed, and material hardness on the resulting surface integrity. Future work will focus on extending the analysis to mechanical and tribological testing, fatigue resistance, and microstructural evaluation. These follow-up studies will establish the relationship between surface topography and functional performance, ensuring that additively manufactured and post-processed components can be reliably applied in engineering practice.

## Acknowledgement

The authors gratefully acknowledge the financial support provided by the Priority Budgetary Research Program (KKTP) of the HUN-REN Centre for Energy Research (EK) under the 2025 funding scheme. This support made the experimental work and analyses presented in this study possible.

**References: 1.** *Leung, Y., Kwok, T., Li, X., Yang, Y., Wang, C. C. L., & Chen, Y.* Challenges and status on design and Computation for emerging additive manufacturing Technologies. Journal of Computing and Information Science in Engineering, 19(2). 2018. https://doi.org/10.1115/1.4041913 **2.** *Zhou, L., Miller, J., Vezza, J., Mayster, M., Raffay, M., Justice, Q., Tamimi, Z. A., Hansotte, G., Sunkara, L. D., & Bernat, J.* Additive Manufacturing: A Comprehensive review. Sensors, 24(9), 2668. 2024. https://doi.org/10.3390/s24092668 **3.** *Nandy, J., Sarangi, H., & Sahoo, S.* A review on Direct Metal Laser sintering: process features and microstructure modeling. Lasers in Manufacturing and Materials Processing, 6(3), 280–316. 2019. https://doi.org/10.1007/s40516-019-00094-y **4.** *Maurya, N. K., Sharma, R., Kumar, N., Kumar, A., Anand, P., Rai, P., & Singh, H.* An overview of investigation of Fatigue, tensile strength and hardness of the components fabricated through direct metal laser sintering (DMLS) process. Materials Today Proceedings, 47, 3979–3984. 2021. https://doi.org/10.1016/j.matpr.2021.04.131 **5.** *Babu, A. S., Jaivignesh, M., Srinivasan, S., & Sugavaneswaran, M.* Design of Functional Gradient Porous Structure and its Fabrication using DMLS Process. Materials Today Proceedings, 24, 1561–1569. 2020. https://doi.org/10.1016/j.matpr.2020.04.476 **6.** *Seharing, A., Azman, A. H., & Abdullah, S.* A review on integration of lightweight gradient lattice structures in additive manufacturing parts. Advances in Mechanical Engineering, 12(6). 2014. https://doi.org/10.1177/1687814020916951 **7.** *Tirnovean, A., Csoregi, N., Borzan, C., & Varga, G.* A REVIEW OF ADDITIVE MANUFACTURING TECHNOLOGIES AND THEIR APPLICATIONS IN THE MEDICAL FIELD. Cutting & Tools in Technological System, 101, 3–16. 2024. https://doi.org/10.20998/2078-7405.2024.101.01 **8.** *Mehdiyev, Z., & Felho, C.* Metal Additive Manufacturing in Automotive Industry: A Review of Applications, Advantages, and Limitations. Materials Science Forum, 1103, 49–62. 2023. https://doi.org/10.4028/p-bg0nin **9.** *Ye, C., Zhang, C., Zhao, J., & Dong, Y.* Effects of post-processing on the surface finish, porosity, residual stresses, and fatigue performance of additive manufactured metals: a review. Journal of Materials Engineering and Performance, 30(9), 6407–6425. 2021. https://doi.org/10.1007/s11665-021-06021-7 **10.** *Patterson, A. E., Messimer, S. L., & Farrington, P. A.* Overhanging features and the SLM/DMLS residual stresses problem: review and future research need. Technologies, 5(2), 15. 2017. https://doi.org/10.3390/technologies5020015 **11.** *Neuberger, H., Hernandez, F., Ruck, S., Arbeiter, F., Bonk, S., Rieth, M., ... & Volker, K. U.* Advances in Additive Manufacturing of fusion materials. Fusion Engineering and Design, 167, 112309. 2021. https://doi.org/10.1016/j.fusengdes.2021.112309 **12.** *Giancarli, L., Chuyanov, V., Abdou, M., Akiba, M., Hong, B., Lässer, R., Pan, C., & Strebkov, Y.* Test blanket modules in ITER: An overview on proposed designs and required DEMO-relevant materials. Journal of Nuclear Materials, 367–370, 1271–1280. 2007. https://doi.org/10.1016/j.jnucmat.2007.03.234 **13.** *Bachmann, C., Ciattaglia, S., Cismondi, F., Eade, T., Federici, G., Fischer, U., Franke, T., Gliss, C., Hernandez, F., Keep, J., Loughlin, M., Maviglia, F., Moro, F., Morris, J., Pereslavtsev, P., Taylor, N., Vizvary, Z., & Wenninger, R.* Overview over DEMO design integration challenges and their impact on component design concepts. Fusion Engineering and Design, 136, 87–95. 2018. https://doi.org/10.1016/j.fusengdes.2017.12.040 **14.** *Day, C., & Murdoch, D.* The ITER vacuum systems. Journal of Physics Conference Series, 114, 012013. 2008. https://doi.org/10.1088/1742-6596/114/1/012013 **15.** *Moon, H., Park, S., Kim, H., & Kim, B. S.* Evaluation of the functional acceptability of the ITER vacuum vessel. Nuclear Fusion, 63(1), 016003. 2022. https://doi.org/10.1088/1741-4326/aca1d0 **16.** *D'Andrea, D.* Additive manufacturing of AISI 316L stainless steel: a review. Metals, 13(8), 1370. 2023. https://doi.org/10.3390/met13081370 **17.** *Zhong, Y., Rännar, L., Liu, L., Koptyug, A., Wikman, S., Olsen, J., Cui, D., & Shen, Z.* Additive manufacturing of

316L stainless steel by electron beam melting for nuclear fusion applications. Journal of Nuclear Materials, 486, 234–245. 2017. https://doi.org/10.1016/j.jnucmat.2016.12.042 **18.** *Gu, D., & Shen, Y.* Processing conditions and microstructural features of porous 316L stainless steel components by DMLS. Applied Surface Science, 255(5), 1880–1887. 2008. https://doi.org/10.1016/j.apsusc.2008.06.118 **19.** *Aziz, U., McAfee, M., Manolakis, I., Timmons, N., & Tormey, D.* A review of optimization of additively manufactured 316/316L stainless steel process parameters, Post-Processing Strategies, and defect mitigation. Materials, 18(12), 2870. 2025. https://doi.org/10.3390/ma18122870 **20.** *Ojo, O. O., & Taban, E.* Post-processing treatments–microstructure–performance interrelationship of metal additive manufactured aerospace alloys: A review. Materials Science and Technology, 39(1), 1–41. 2022. https://doi.org/10.1080/02670836.2022.2130530 **21.** *Kaynak, Y., & Kitay, O.* Porosity, Surface Quality, Microhardness and Microstructure of Selective Laser Melted 316L Stainless Steel Resulting from Finish Machining. Journal of Manufacturing and Materials Processing, 2(2), 36. 2018. https://doi.org/10.3390/jmmp2020036 **22.** *Guzanová, A., Ižaríková, G., Brezinová, J., Živčák, J., Draganovská, D., & Hudák, R.* Influence of Build Orientation, Heat Treatment, and Laser Power on the Hardness of Ti6Al4V Manufactured Using the DMLS Process. Metals, 7(8), 318. 2017. https://doi.org/10.3390/met7080318 **23.** *Melia, M. A., Duran, J. G., Koepke, J. R., Saiz, D. J., Jared, B. H., & Schindelholz, E. J.* How build angle and post-processing impact roughness and corrosion of additively manufactured 316L stainless steel. Npj Materials Degradation, 4(1). 2020. https://doi.org/10.1038/s41529-020-00126-5 **24.** *Diniță, A., Neacșa, A., Portoacă, A. I., Tănase, M., Ilinca, C. N., & Ramadan, I. N.* Additive Manufacturing Post-Processing Treatments, a Review with Emphasis on Mechanical Characteristics. Materials, 16(13), 4610. 2023. https://doi.org/10.3390/ma16134610 **25.** *Romanescu, P., Omidvarkarjan, D., Ferchow, J., & Meboldt, M.* Evaluation of the Ultra-High Vacuum Suitability of Laser Powder Bed Fusion Manufactured stainless steel 316L. In Springer tracts in additive manufacturing (pp. 407–422). 2023. https://doi.org/10.1007/978-3-031-42983-5_27

Іштван Станкович, Мішкольц, Угорщина, Габор Вереш, Будапешт, Угощина, Чаба Фельхо, Антал Надь, Мішкольц, Угорщина, Петер Фігецькі-Мелюкуті, Будапешт, Угорщина

# ВПЛИВ ПОСТОБРОБКИ НА ОСНОВІ МЕХАНІЧНОЇ ОБРОБКИ НА ТОПОГРАФІЮ ПОВЕРХНІ НЕРЖАВІЮЧОЇ СТАЛІ DMLS 316L ДЛЯ ЗАСТОСУВАНЬ, ПОВ'ЯЗАНИХ З ПЛАВЛЕННЯМ

**Анотація.** *У цьому дослідженні досліджується вплив постобробки на основі механічної обробки на топографію поверхні нержавіючої сталі Direct Laser Sintered (DMLS) 316L, призначеної для застосувань, пов'язаних із термоядерним синтезом. Кубічні зразки (30 × 30 × 30 мм) виготовлялися методом адитивного виробництва і в подальшому допрацьовувалися торцевим фрезеруванням і шліфуванням поверхні при двох параметричних налаштуваннях кожен. Рельєф поверхні був охарактеризований за допомогою оптичної системи AltiSurf 520 відповідно до стандарта ISO 25178. Надрукована поверхня продемонструвала високу шорсткість (Sa = 8,899 мкм, Sz = 79,427 мкм), тоді як усі поверхні, що пройшли постобробку, показали значне покращення. Найнижча шорсткість (Sa = 1,346 мкм) була отримана після шліфування при швидкості подачі 7 м/хв. Аналіз перекосу та куртозу показав, що механічна обробка перетворила поверхню, в більш однорідну, майже гаусову текстуру. Результати підтверджують, що контрольовані операції фрезерування та шліфування можуть ефективно покращити цілісність поверхні компонентів DMLS 316L. Ці результати демонструють потенціал гібридного адитивно-субтрактивного виробництва для отримання поверхонь, придатних для вакуума та функціональних вимог застосування термоядерних технологій. У цьому контексті дослідження підтверджує*

*життєздатність інтеграції 3D-друку як підготовчого етапу у виробництві компонентів, що вимагають специфічної функціональності поверхні після фінішної обробки. Однак, оскільки це було попереднє дослідження, необхідні подальші дослідження, щоб повністю перевірити технологічний ланцюжок і вивчити вплив додаткових змінних, таких як геометрія інструменту, швидкість різання та твердість матеріалу, на результуючу цілісність поверхні. Майбутня робота буде зосереджена на поширенні аналізу на механічні та трибологічні випробування, стійкість до втоми та оцінку мікроструктури. Ці подальші дослідження встановлять взаємозв'язок між топографією поверхні та функціональними характеристиками, гарантуючи, що компоненти, виготовлені адитивно та після обробки, можуть бути надійно застосовані в інженерній практиці.*

**Ключові слова:** *адитивне виробництво; нержавіюча сталь DMLS 316L; рельєф поверхні; постобробка; застосування технології термоядерного синтезу.*